Perfluoroalkyl [70]-Fullerenes as Robust Highly-Luminescent Fluorocarbons, or Position of One CF3 Group Matters

ARTICLE *in* JOURNAL OF PHYSICAL CHEMISTRY LETTERS · JULY 2013

Impact Factor: 7.46 · DOI: 10.1021/jz401068t

6 AUTHORS, INCLUDING:

Yuhuan Jin
Nalco Company
9 PUBLICATIONS **103** CITATIONS
SEE PROFILE

Olga V. Boltalina
Colorado State University
268 PUBLICATIONS **4,252** CITATIONS
SEE PROFILE

Alexey A Popov
Leibniz Institute for Solid State and Materials …
188 PUBLICATIONS **3,412** CITATIONS
SEE PROFILE

THE JOURNAL OF PHYSICAL CHEMISTRY Letters

Letter

pubs.acs.org/JPCL

Perfluoroalkyl [70]-Fullerenes as Robust Highly-Luminescent Fluorocarbons, or Position of One CF_3 Group Matters

Karlee P. Castro,[†] Yuhuan Jin,[‡] Jeffrey J. Rack,*[,‡] Steven H. Strauss,*[,†] Olga V. Boltalina,*[,†] and Alexey A. Popov*[,§]

[†]Department of Chemistry, Colorado State University, Fort Collins, Colorado 80523, United States

[‡]Department of Chemistry and Biochemistry, Ohio University, Athens, Ohio 45701, United States

[§]Department of Electrochemistry and Conducting Polymers, Leibniz Institute for Solid State and Materials Research, D-01069 Dresden, Germany

Supporting Information

ABSTRACT: The photophysical properties of two $C_{70}(CF_3)_8$ and three $C_{70}(CF_3)_{10}$ isomers were studied using steady-state and time-resolved absorption and fluorescence spectroscopy. Four of the compounds exhibited quantum yields (Φ_F) higher than for any C_{70} derivative reported to date, and three exceeded 0.24, the highest Φ_F reported for any fullerene or fullerene derivative. A difference in the location of only one CF_3 group in $C_{70}(CF_3)_8$ and $C_{70}(CF_3)_{10}$ isomers resulted in 200-fold and 14-fold increases in Φ_F, respectively. The isomer of $C_{70}(CF_3)_{10}$ with the highest Φ_F (0.68 in toluene) also exhibited the longest fluorescence lifetime, 51 ns, thus competing favorably in its luminescent properties with the most luminescent carbon materials studied to date. Formation of the S_1 state in one of the $C_{70}(CF_3)_{10}$ isomers occurred within 0.6 ps and its nanosecond-long decay was monitored by ultrafast transient absorption spectroscopy. Time-dependent density functional theory calculations were performed to provide a physically meaningful understanding of the photophysical properties of $C_{70}(CF_3)_n$ derivatives.

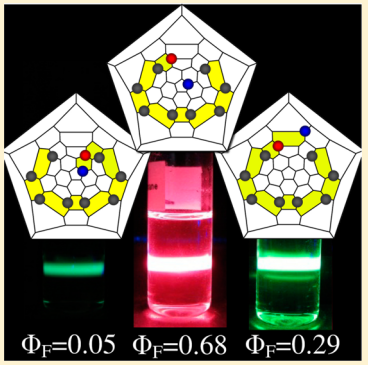

SECTION: Physical Processes in Nanomaterials and Nanostructures

The third wave of the booming interest in the carbonaceous materials, following the initial fullerene wave and the second carbon nanotube (CNT) wave, is focused on graphene and related structures. Their photoluminescence (among many other interesting optoelectronic properties beyond the scope of this work) offers several promising applications. Graphene itself is a zero-gap material and hence nonluminescent. Conceptually, however, "graphene" luminescence can be induced by rolling it into carbon nanotubes,[1,2] by introducing defects (i.e., by chemical modification to produce graphene oxide[3,4]), or by limiting the size of the π-system (i.e., reducing the size of the graphene sheet[5,6]). The latter approach leads to so-called graphene quantum dots (GQDs), a subclass of carbon quantum dots (CQDs).

Fabrication and characterization of GQDs and CQDs has been a matter of intense research in the past years.[5−9] Optical properties of the materials with confined excitons (such as quantum dots) depend on the spatial extension of the exciton and hence can be tuned by varying the size of the system.[10] In spite of the impressive progress in the fabrication of GQDs with defined size and optical properties, control of their size distribution still remains a challenge. Not surprisingly, the best control over the properties of GQDs is possible when they are synthesized by a bottom-up approach in well-controlled chemical steps. Organic solution-based chemistry allows the synthesis of luminescent GQDs comprising 100−200 carbon atoms.[8] Thus, on the small end of the size distribution, GQDs are approaching the size of common fullerenes. In fact, taking into account the difficulties in controlling GQD size and structure, fullerenes as constant-composition *molecular* materials have several obvious advantages. First, their separation from one another can be achieved by well-established chromatographic techniques. Second, well-defined molecular structures and π-system topology have been revealed for many fullerenes by ^{13}C NMR spectroscopy and single-crystal X-ray structures. Third, multiple cage isomers with different electronic properties are known for nearly all fullerenes with more than 70 carbon atoms. Fourth, fullerenes do not undergo graphitization via stacking (this limits the size of genuine single-layer GQDs). Despite these advantages and the photophysical properties that could potentially make fullerenes useful in photodynamic therapy or electroluminescence applications,[11−13] fullerenes have remained in the shadows and are barely mentioned when luminescent carbonaceous materials are considered because of their very weak fluorescence. The fullerenes C_{60} and C_{70} have dipole-forbidden $S_0 \leftrightarrow S_1$ transitions,[14] which lead to small values of radiative decay constants (e.g., $k_F = 2.7 \times 10^5$ s^{-1} for C_{60} and 8.8×10^5 s^{-1} for C_{70}), in agreement with the Strickler−

Received: May 23, 2013
Accepted: July 10, 2013
Published: July 10, 2013

Berg rule.[15] Furthermore, both fullerenes show high rates of intersystem crossing with almost quantitative formation of a triplet state. These two factors result in short fluorescence lifetimes (e.g., τ_F = 1.2 ns for C_{60} and 0.7 ns for C_{70}) and very low fluorescence quantum yields (e.g., Φ_F = ca. 0.0003 for C_{60} and ca. 0.0006 for C_{70} in toluene).[15−19] For comparison, GQD Φ_F values can be as high as 0.28,[20] and the most luminescent carbon quantum dots have Φ_F values as high as 0.80.[21]

Derivatization of the fullerenes reduces the symmetry and changes their π-system. Thus, absorptions of the derivatives are usually optically allowed and hence higher values of k_F can be reached. However, the relatively small perturbation of the fullerene π-system at early stages of functionalization preserves the low $S_0 \rightarrow S_1$ absorption intensities and efficient intersystem crossing and leads to relatively low Φ_F values.[22−24] More extensive derivatization, *in some cases*, changes the fullerene π-system enough to lead to much higher Φ_F values. For example, Nakamura et al. reported a 0.24 Φ_F value for $C_{60}Ph_{10}(CH_2Ph)_3Me_2H$ (see Figure 1), much higher than for

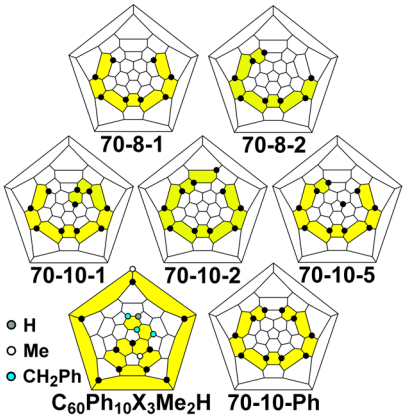

Figure 1. The top two rows of Schlegel diagrams represent the $C_{70}(CF_3)_8$ and $C_{70}(CF_3)_{10}$ isomers studied in this work. The bottom row shows the Schlegel diagrams of $C_{60}Ph_{10}(CH_2Ph)_3Me_2H$ (Φ_F = 0.24[25]) and $C_{70}Ph_{10}$ (**70−10-Ph**; Φ_F = 0.025[26]). The black dots denote the positions of the cage C atoms bearing the CF_3 or Ph groups.

any previously reported fullerene derivative.[25] However, even with 10 substituents, the Φ_F value for $C_{70}Ph_{10}$ is only 0.025 (Schlegel diagrams of $C_{60}Ph_{10}(CH_2Ph)_3Me_2$ and $C_{70}Ph_{10}$ are shown in Figure 1).[26] Photophysical studies of $C_{70}Ph_n$ derivatives (n = 4−10) showed that intersystem crossing is the primary mechanism of S_1 decay, and even for the strongest fluorophore in the series, $C_{70}Ph_{10}$, the yield of the triplet state is nearly quantitative.[26,27] Note that 0.025 is the highest Φ_F value reported for any C_{70} derivative until this work.

During the past decade, perfluoroalkylation has been established as a versatile tool for the synthesis of multiply functionalized fullerene derivatives with well-defined molecular structures.[28−33] Trifluoromethylfullerenes (TMFs) exhibit a number of useful properties, which are absent in many other carbonaceous nanostructures such as GQDs. First, TMFs are thermally stable, which allows them to be used in high-temperature applications. Second, TMFs can be sublimed without decomposition, so high-quality thin films can be fabricated by vapor-deposition. They are freely soluble in many organic solvents, allowing films to be fabricated by spin-casting or spray methods. Third, libraries of TMFs with different numbers of CF_3 groups and different isomeric structures for a given number of CF_3 groups can be prepared in a single reaction followed by one- or two-step HPLC separation. Perfluoroalkyl-derivatives were already synthesized and structurally characterized for many fullerenes reaching the size of C_{96}[34−38] and there are no conceptual difficulties in applying these techniques to even larger fullerenes. Besides, perfluoroalkylation of PAHs, corannulene, CNTs, and graphite nanosheets has been explored recently.[39−43] Importantly, the addition patterns (i.e., the sets of CF_3 group locants on the fullerene surface) are precisely known by ^{19}F NMR spectroscopy and single-crystal X-ray structures for the majority of the more than 100 known TMFs. Finally, electrochemical studies of 18 $C_{60}(CF_3)_n$ and 17 $C_{70}(CF_3)_n$ derivatives with n = 2−12 showed that varying the value of n and, even more importantly, varying the addition pattern for a given value of n, allows for versatile tuning of their electronic properties (e.g., the ranges of first reduction potentials for $C_{60}(CF_3)_n$ and $C_{70}(CF_3)_n$ compounds are 0.73 and 0.45 V, respectively).[30,33]

In this work we report on the first photophysical studies of $C_{70}(CF_3)_n$ derivatives. We have found that $C_{70}(CF_3)_8$ and $C_{70}(CF_3)_{10}$ derivatives with different addition patterns exhibit significantly different photophysical properties. Isomers differing in the placement of only one CF_3 group have very different Φ_F values. One particular $C_{70}(CF_3)_{10}$ isomer has a Φ_F value of 0.68 in toluene, nearly 3 times higher than for any fullerene derivative or GQD, making it the brightest fullerene fluorophore ever studied. Importantly, these results can be understood with the use of new time-dependent density functional theory (TD-DFT) calculations.

Steady State Measurements. The Schlegel diagrams for the $C_{70}(CF_3)_8$ and $C_{70}(CF_3)_{10}$ derivatives studied in this work are shown in Figure 1 (their molecular structures were determined earlier).[29−31] The compounds **70−8−1**, **70−8−2**, **70−10−1**, **70−10−2**, and **70−10−5** were isolated from the products of high-temperature reactions of C_{70} with CF_3I in a flow-tube apparatus[28] or a gradient-temperature gas−solid reactor.[44] The compounds **70−10−2** and **70−10−5** were previously produced in small quantities with low yields.[30] The use of the gradient-temperature gas−solid reactor increased the yields of these compounds by ca. a factor of 5 (see SI for details on isolation and characterization of $C_{70}(CF_3)_{8-10}$ compounds).

Absorption and fluorescence spectra of **70−8−2** in cyclohexane and **70−10−1**, **70−10−2**, and **70−10−5** in toluene are shown in Figure 2. The spectra of **70−8−1** in cyclohexane are shown in the Supporting Information (SI). Table 1 lists the principal spectroscopic parameters. All of the compounds exhibited fluorescence spectra with well-defined vibronic structure comprising the 0−0 transition and its 2−3 descending equidistant replicas, each at ca. 1350 cm^{-1}. These features were well matched by the analogous bands in the lowest-energy part of the absorption spectra, showing that the mirror-image rule is fulfilled and enabling precise determination of the energies of the first excited singlet states. The energies show a weak but distinct solvent shift of 100−300 cm^{-1}; the S_1 energies for toluene solutions were lower than for cyclohexane solutions. The Stokes shifts are relatively small and span the range 90−650 cm^{-1}. The largest shifts were found for toluene solutions, and the smallest for cyclohexane solutions. The compound **70−10−1** was the only compound that showed an apparent deviation from the mirror-image rule. Its absorption spectrum has no distinct vibronic structure, presumably due to the

dx.doi.org/10.1021/jz401068t | J. Phys. Chem. Lett. 2013, 4, 2500−2507

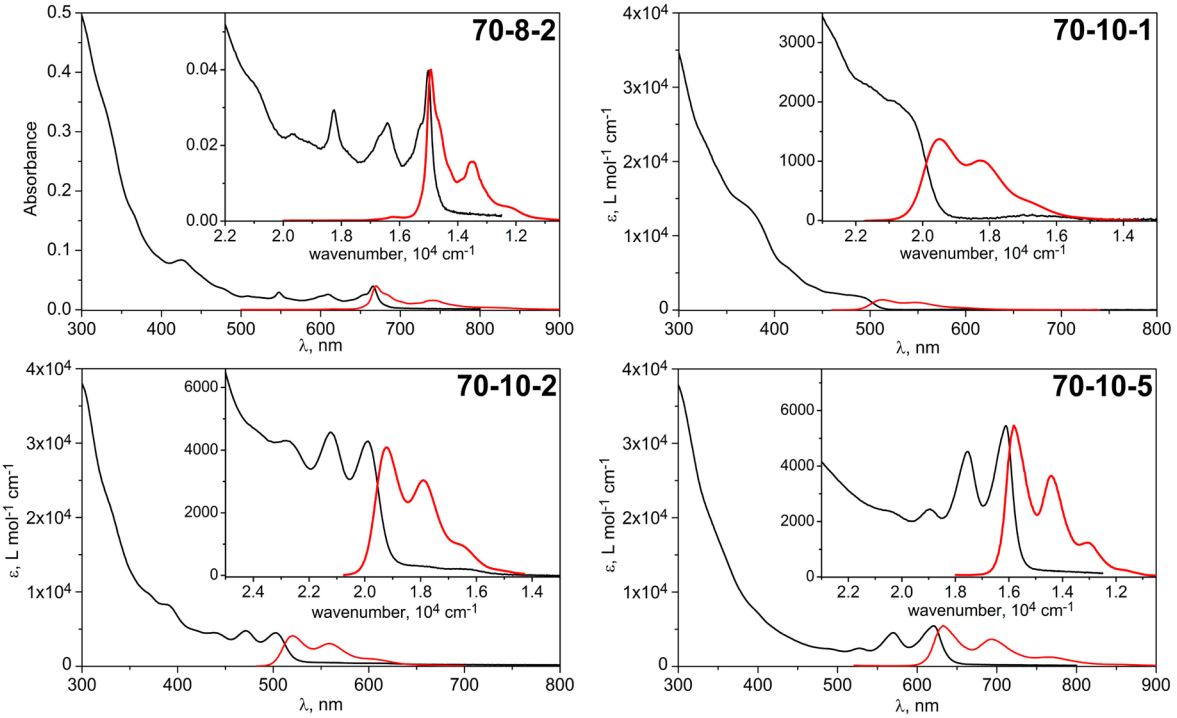

Figure 2. Absorption (black) and fluorescence (red) spectra of **70−8−2** (λ_{ex} = 444 nm), **70−10−1** (λ_{ex} = 449 nm), **70−10−2** (λ_{ex} = 468 nm), and **70−10−5** (λ_{ex} = 570 nm). Molar absorption coefficients (ε) at the excitation wavelengths are 3.2 × 10^3 (**70−10−1**), 9.7 × 10^3 (**70−10−2**), and 5.2 × 10^3 L mol^{-1} cm^{-1} (**70−10−5**). The insets show vertically expanded spectra for the lowest energy absorption and fluorescence bands. The wavenumber scale is used in the insets to more readily provide visual evidence of the mirror-image rule.

Table 1. Absorption and Emission Maxima (λ), Stokes Shifts (Δ), Fluorescence Quantum Yields (Φ_F), Fluorescence Lifetimes (τ_F), and Fluorescence Decay Rate Constants (k_F) for $C_{70}(CF_3)_8$ and $C_{70}(CF_3)_{10}$ Compounds in Different Solvents[a]

cmpd	solv	λ_{abs} nm	λ_F nm	Δ^b cm^{-1}	$\Phi_F{}^c$	τ_F ns	10^6 k_F s^{-1}
70−8−1	chx	595	613	495	0.0012	–	–
70−8−2	chx	666	670	90	0.27	–	–
70−10−1	chx	–	506	–	0.041	4.0	10.2
	tol	–	513	–	0.047	5.6	8.4
70−10−2	chx	499	514	585	0.24	4.5	53.3
	tol	503	520	650	0.29	3.2	90.6
70−10−5	chx	616	623	182	0.50	54.7	9.1
	tol	621	632	280	0.68	50.9	13.4

[a]Solvents are abbreviated as follows: chx − cyclohexane, tol − toluene. [b]Δ denotes the Stokes shift. [c]The uncertainties in Φ_F values are ≤10% except for **70−8−1**, for which the uncertainty may be higher than 100% because of its low fluorescence intensity.

overlap with higher-energy excitations (see SI), and its Stokes shift could not be determined precisely.

Although all of the $C_{70}(CF_3)_n$ derivatives studied in this work have a common addition-pattern motif (i.e., a belt of 8 CF_3 groups around the C_{70} equator), the Φ_F values vary from 0.0012 to 0.68, demonstrating that small addition-pattern variations can have very large effects. Both **70−8−1** (C_s symmetry) and **70−8−2** (C_2 symmetry) have addition patterns that can be described as a ribbon of seven edge-sharing $C_6(CF_3)_2$ hexagons, and differ by the position of only one CF_3 group. Nevertheless, this change results in the increase of Φ_F from 0.0012 to 0.24, respectively. A similar situation was found for the $C_{70}(CF_3)_{10}$ isomers. The structure of **70−10−5** is related to the structures of **70−10−1** and **70−10−2** by the position of one CF_3 group (a different one in each case), but these seemingly small structural differences are sufficient to change Φ_F from 0.05 for **70−10−1** to 0.25 for **70−10−2** to 0.68 for **70−10−5**. The latter value is now the highest value reported for any fullerene derivative and is almost 3 times larger than the 0.24 value for previous record holder, $C_{60}Ph_{10}(CH_2Ph)_3(CH_3)_3H$.[25] Furthermore, the addition patterns of **70−10−5** and $C_{70}Ph_{10}$ also differ by the position of only one substituent, but their Φ_F values differ by more than 50 times, 0.68 for **70−10−5** and 0.025 for $C_{70}Ph_{10}$.[26] That this Φ_F disparity is due to the minor addition-pattern difference and not to the electronic or steric properties of the CF_3 and Ph substituents is shown by comparing the Φ_F values in cyclohexane for **70−8−1** (0.0012) and $C_{70}Ph_8$ (0.013 ± 0.005[26]). It is now apparent that the luminescence efficiencies and the highest occupied molecular orbital to lowest unoccupied molecular orbital (HOMO−LUMO) gaps of $C_{70}(CF_3)_n$ derivatives, and not only their reduction potentials,[30] can be conveniently tuned by the proper choice of addition pattern.

Time-Resolved Measurements. Further insight into the photophysical properties of the $C_{70}(CF_3)_n$ derivatives was obtained by time-resolved measurements using 355 nm excitation from a pulsed Nd:YAG laser. The fluorescence lifetimes (τ_F) listed in Table 1 show that **70−10−5** has the longest lifetimes, 51 ns in toluene and 55 ns in cyclohexane, as well as the highest quantum yields, 0.68 in toluene and 0.50 in cyclohexane. Its lifetime in toluene is more than 70 times longer that that of C_{70} in toluene (0.7 ns[19]) and is close to the 67 ns lifetime reported by Nakamura et al. for $C_{60}Ph_5(p\text{-}C_6H_4(^tBu)_5Me_2$, which has a cyclophenacene-like π-system and a Φ_F value of 0.185.[13]

dx.doi.org/10.1021/jz401068t | J. Phys. Chem. Lett. 2013, 4, 2500−2507

The excited state behavior of these compounds was also studied by ultrafast transient absorption spectroscopy. Due to solubility limitations, only **70−10−2** could be studied in perfluorodecalin at this time. It was excited at 495 nm, which corresponds to the lowest energy absorption maximum in this solvent. Figure 3 shows transient absorption spectra recorded at

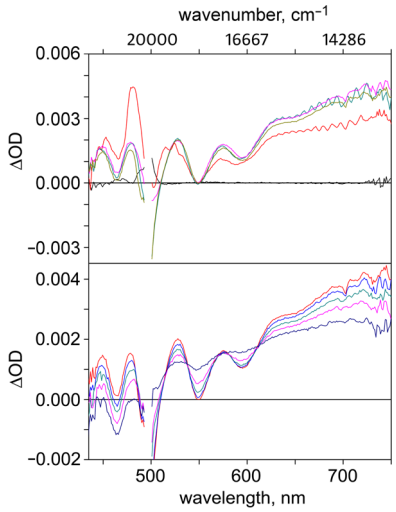

Figure 3. Transient absorption spectra of **70−10−2** in perfluorodecalin measured at different pump−probe delays. Top panel: −0.07 ps (black); 0.30 ps (red); 0.520 ps (blue); 1.97 ps (purple); 99.9 ps (green). Bottom panel: 99.9 ps (red); 299 ps (blue); 605 ps (green); 1.200 ns (purple); 2.99 ns (navy).

different pump−probe delays. At delays shorter than 2 ps, the spectra exhibit an almost instantaneous rise throughout the visible region characterized by several absorption features and a shallow bleach (i.e., a negative peak) near 500 nm. The negative peak is ascribed to loss of the ground state, while the absorption bands are ascribed to the $S_1 \rightarrow S_n$ excited state transitions. This evolution was complete within 0.6 ps, and this state persisted for the next 100 ps.

More dramatic changes in the transient absorption spectra occurred at longer pump−probe delays. From 100 to 2990 ps, the spectra reveal an evolution from one electronic state to another with the emergence of four isosbestic points at 516, 537, 576, and 612 nm. The spectrum at 2990 ps exhibits broad features at long wavelengths and sharp, narrow features from 440 to ca. 490 nm. The broad features are consistent with a triplet excited state. Based on our computational results, described in the next section, we ascribe the longer-time spectral changes to the conversion of the S_1 state to a T_1 state. Kinetic data at multiple wavelengths and a global fitting analysis revealed a lifetime of 1270 ± 150 ps, which is consistent with literature values for other fullerenes and their derivatives.[45−51] This lifetime is shorter by a factor of 2−3 as determined by fluorescence spectroscopy in cyclohexane or toluene solution. We tentatively ascribe this difference in the measured lifetime to unspecified solvent interactions. We also found that the relaxed S_1 state was formed within 0.6 ps.

The transient absorption spectra in Figure 3 are also consistent with a number of other studies on fullerenes (we are not aware of any transient absorption spectra for C_{70} derivatives).[45−47,49,51] Of particular note is that many previous studies show an increase in the absorption of the excited state relative to the ground state. However, few of these studies show the absorption detail that we find here. It is not certain yet if these peaks are due to more allowed transitions associated with the trifluoromethylated C_{70} studied here, or if it is due to differences in the spectral resolution of the instruments employed. However we note that the ground state absorption spectrum of **70−10−2**, shown in Figure 2, features low energy peaks separated by ca. 1500 cm^{-1}. For comparison, the transient absorption spectrum at a 2 ps delay (ascribed to $S_1 \rightarrow S_n$) exhibits peaks separated by 1351 cm^{-1} (449 nm, 498 nm) and 1578 cm^{-1} (520 nm, 576 nm). It is likely that these peaks are due to the vibrational structure of the S_1 state. Our future studies will include efforts to understand the excited state electronic structures of these and related compounds.

Computational Studies. To understand the reasons for the large variation in Φ_F values measured in this work, and to propose addition patterns for fullerene derivatives with even higher quantum yields, we performed TD-DFT calculations at the PBE/TZ2P level. The fluorescence quantum yield is related to the radiative and nonradiative decays of the S_1 state via the equation $\Phi_F = k_F/(k_F + k_{nr})$. To achieve the maximum quantum yield, the fluorescence rate constant k_F should be maximized, and the cumulative rate constant of nonradiative processes, k_{nr}, should be minimized.

Table 2. Experimental and Calculated S_1 and T_1 Energies and $S_0 \rightarrow S_1$ Oscillator Strengths f[a]

	C_{70}	70−8−1	70−8−2	70−10−1	70−10−2	70−10−5
S_1-exp	1.93	2.02	1.86	2.42	2.38	1.96
S_1-vert	1.75	1.83	1.51	2.19	2.03	1.62
S_1-adb	1.69	1.62	1.43	2.05	1.89	1.51
f_{exp}-int					0.039	0.046
f_{exp}-SB				0.015	0.162	0.035
f_{calc}	0.000	0.003	0.012	0.011	0.036	0.041
τ_F-exp				5.6	3.2	50.9
τ_F-calc		1.1	72.7	7.8	12.1	45.9
T_1-adb	1.52	1.37	0.98	1.75	1.38	1.03
$\Delta_{S1\text{-}T1}$	0.16	0.25	0.44	0.29	0.51	0.48
$T_1 \rightarrow T_2$-vert		0.63	0.72	0.46	0.73	0.79

[a]All energies are in eV; S_1-exp is the energy of S_1 from fluorescence in toluene, S_1-vert and S_1-adb are vertical and adiabatic $S_0 \rightarrow S_1$ excitation energies computed at the TD-PBE/TZ2P level; f_{exp}-int and f_{exp}-SB are oscillator strengths determined experimentally by integration of the absorption spectrum (int) or from Strickler−Berg relation (SB) using experimental k_F values; f_{calc} denotes TD-DFT computed oscillator strengths; τ_F-exp are experimental lifetimes, τ_F-calc are lifetimes computed using experimental Φ_F and computed f values.

dx.doi.org/10.1021/jz401068t | J. Phys. Chem. Lett. 2013, 4, 2500−2507

The Strickler–Berg (SB) rule connects k_F with the absorption intensity:[52,53]

$$k_F = 2900 \cdot n^2 \nu_{max}^2 \int_{S_0 \rightarrow S_1} \epsilon d\nu = 0.125 \cdot n^2 \nu_{max}^2 f$$

where n is a refractive index of the solvent, ν_{max} is absorption maximum (in 10^4 cm^{-1}), and f is the oscillator strength of the $S_0 \rightarrow S_1$ excitation. According to the SB rule, high fluorescence rate constant is expected for the molecules with high oscillator strength. Very good matches between the f values, listed in Table 2, that were obtained by direct integration of the absorption spectrum and from the k_F value determined in photophysical measurements shows that the SB rule holds for **70–10–5**. At the same time, **70–10–2** significantly deviates from the rule (its k_F value is ca. 4 times higher than might be expected from the SB equation). The values listed in Table 2 show that the TD-PBE method underestimates excitation energies (adiabatic values by ca. 0.4 eV; vertical values by ca. 0.25 eV), but relative S_1 energies and, even more importantly, computed oscillator strengths agree very well with the experimental estimations. For **70–10–1**, the f value computed from the SB equation also fits the TD-DFT prediction very well. Hence, it is reasonable to use computed f values when their experimental determination is not possible, and then estimate the lifetimes using the experimental quantum yields. Comparison of the f values for **70–8–1** and **70–8–2** shows that their Φ_F difference can be explained, in part, by the very low oscillator strength of the $S_0 \rightarrow S_1$ excitation in **70–8–1**. By contrast, very long lifetimes would be expected for **70–8–2**. In principle, it appears that compounds with higher Φ_F tend to have higher oscillator strengths. However, the analysis of only f is not sufficient to explain our results because, for example, **70–8–2** and **70–10–1** have similar f values for their respective $S_0 \rightarrow S_1$ excitations but have quantum yields that differ by more than a factor of 6.

Analysis of the rate of the nonradiative decay is more complicated and its direct prediction is hardly possible now. However, if $S_1 \rightarrow T_1$ intersystem crossing (ISC) remains the main pathway for the nonradiative decay, the energy-gap law can be applied, which states that the rate of the ISC increases with the decrease of the energy gap between the states, Δ_{S1-T1}.[53] The Δ_{S1-T1} values listed in Table 2 show that the largest gap of 0.5 eV is found for **70–10–2** and **70–10–5** followed by **70–8–2** with 0.44 eV. In the series **70–10–1** to **70–8–1** to C_{70} the Δ_{S1-T1} values decrease from 0.29 to 0.25 to 0.16 eV. Thus, it is clear that compounds with high fluorescence yield have the largest Δ_{S1-T1} gaps. To verify that $S_1 \rightarrow T_2$ ISC is unlikely, we have also computed vertical $T_1 \rightarrow T_2$ excitation energies and found that in all compounds T_2 state is higher in energy than S_1.

Increase of the fluorescence yields for multiply functionalized C_{60} derivatives was earlier ascribed to the shrinking of the π-system.[13,25] Our results show that neither the size nor the location of the π-system itself is of such a high importance since there remain 60 $C(sp^2)$ atoms in very similar positions in the three $C_{70}(CF_3)_{10}$ isomers. Presumably, the spatial extension of the $S_0 \rightarrow S_1$ excitation, which is visualized in Figure 4 by plotting the difference S_1/S_0 electron densities, is a factor that also plays a role. Larger Δ_{S1-T1} gaps are achieved when excitation is more localized (i.e., when the HOMO and LUMO are spatially localized in the same fragment of the molecule), as in **70–10–2** and **70–10–5**, whereas a larger spatial extension leads to smaller Δ_{S1-T1} gaps as in **70–10–1**. Since the addition pattern dictates the shape and localization of the frontier orbitals in functionalized fullerenes, including TMFs,[33] it follows that it should also determine their photophysical properties, as we have shown in this study.

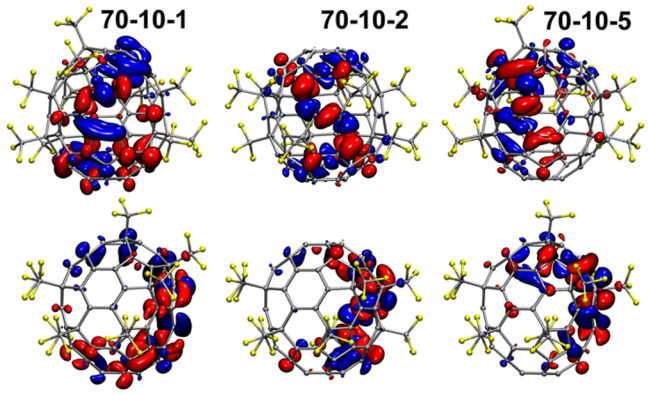

Figure 4. TD-DFT computed difference electronic densities for $S_0 \rightarrow S_1$ excitation, $\Delta\rho = \rho(S_1) - \rho(S_0)$, in **70–10–1**, **70–10–2**, and **70–10–5**. Positive and negative $\Delta\rho$ lobes (i.e., spatial distribution of the electron and hole in the exciton formalism) are red and blue, respectively. Each molecule is shown in two orientations in the top and bottom rows.

To summarize, this work shows that perfluoroalkylation is a versatile tool for the band gap engineering and tuning of the luminescent properties of fullerenes (and presumably other carbonaceous materials). We have found that in contrast to the nonluminescent parent C_{70}, $C_{70}(CF_3)_n$ compounds can be strong fluorophores, the quantum yields of which are strongly dependent on the addition patterns and can be as high as 0.68, several times higher than any reported fullerene derivative or GQD. The highest quantum yields were found for the compounds with (i) the largest oscillator strengths of the $S_0 \rightarrow S_1$ transition and (ii) the largest Δ_{S1-T1} gaps. These two quantities can be straightforwardly predicted by TD-DFT computations, simplifying the search for the most promising compounds among many dozens of possible fullerene$(CF_3)_n$ derivatives.

Experimental Details. The five TMFs studied in this work were purified by HPLC (Nacalai Tesque Cosmosil Buckyprep semipreparative column (250 × 10 mm i.d.), Shimadzu Prominence HPLC system, LC-8A pump, 20 mL sample loop, SPD-M20A diode array detector, DGU-20As degasser, CBM-20A communications bus module, and FRC-10A fraction collector). TMF purity was shown to be 95 mol % or higher as shown by ^{19}F NMR spectroscopy (Varian 400 spectrometer). UV–vis spectra were obtained on a Cary 500 UV–vis–NIR spectrometer.

Steady-state fluorescence was measured on an AVIV ATF-105 Auto-Titrating Differential/Ratio Spectrofluorimeter with a 90° measurement geometry. The standard used was 4-(dicyanomethylene)-2-methyl-6-(4-dimethylaminostyryl)-4H-pyran (DCMP; Sigma-Aldrich) dissolved in absolute ethanol (Pharmco-Aaper), which has a published value of 0.44 ± 0.02.[54] The samples were dissolved in cyclohexane (Mallinckrodt) or toluene (Burdick and Jackson).

Sample solutions were degassed with a minimum of three freeze–pump–thaw cycles. The cuvette size was 1 cm square. Each solution was measured three times. A blank solution of the pure solvent was also measured three times for each sample or standard solution. The absorbance of standard and sample were matched at the excitation wavelength and the absorbance

dx.doi.org/10.1021/jz401068t | J. Phys. Chem. Lett. 2013, 4, 2500–2507

at and above the excitation wavelength was kept below 0.1. Slit widths were 2 nm, the step size was 1 nm, and the temperature was 25 ± 0.2 °C. The spectra were corrected for wavelength dependent detector response using a correction curve generated by comparing the measured spectrum of tetraphenylporphyrin with published data.[55,56] To ensure correct determination of fluorescence intensities in the NIR range, additional fluorescence measurements were performed on a homemade system comprising a 405 nm laser (Omicron) and an Avantes AvaSpec-ULS2048XL diode-array spectrometer. The detector was calibrated with an Avantes AvaLight-DH-CAL certified halogen lamp. Corrected spectra measured independently on both systems were found to be virtually identical.

Fluorescence quantum yields were calculated using the equation:

$$\Phi_x = \Phi_{std}\left(\frac{\int F_x}{\int F_{std}}\right)\left(\frac{1 - 10^{-A_{std}}}{1 - 10^{-A_x}}\right)\left(\frac{\eta_x^2}{\eta_{std}^2}\right)$$

where x represents the sample, std represents the standard, Φ is the quantum yield, $\int F$ is the integrated fluorescence intensity, A is the absorbance at the excitation wavelength, and η is the refractive index of the solvent.

Fluorescence lifetimes were measured with an Edinburgh LP920 Spectrometer equipped with an Edinburgh TM300 monochromator and an Edinburgh LP900 PMT using a Surelite Continuum Nd:YAG laser with a Surelite SSP. The excitation wavelength was 355 nm. Detection occurred near the fluorescence emission maximum. During the measurements, two laser pulses were discarded, and three were averaged for one output. The instrument response was also recorded for each sample using a 1-cm cuvette filled with the relevant solvent. Using Edinburgh L900 software, a reconvolution fit was calculated using the sample signal and the instrument response. From this fit, the fluorescence lifetime of the sample was determined. Samples were measured in the same solvents as those used in the fluorescence quantum-yield measurements. For ultrafast transient absorption measurements, excitation was at 495 nm and a sapphire crystal was employed to generate the white light continuum with a detection range of ca. 450 to 800 nm

TD-DFT was performed with the PBE functional and TZ2P basis set using the Prioda code.[57,58] The difference densities in Figure 4 were visualized using the VMD code.[59]

■ ASSOCIATED CONTENT

Ⓢ Supporting Information

Details of synthesis, spectroscopic data, and TD-DFT excitations energies. This material is available free of charge via the Internet at http://pubs.acs.org.

■ AUTHOR INFORMATION

Corresponding Author

*E-mail: a.popov@ifw-dresden.de (A.A.P.); rackj@ohio.edu (J.J.R.); ovbolt@lamar.colostate.edu (O.V.B.); steven.strauss@colostate.edu (S.H.S.).

Notes

The authors declare no competing financial interest.

■ ACKNOWLEDGMENTS

We are grateful to the NSF for Grants CHE-1012468 to O.V.B. and S.H.S. and CHE-0947031/CHE-1112250 to J.J.R. Y.J. thanks Ohio University for a Clippinger Graduate Fellowship. A.A.P. acknowledges the DFG (PO 1602/1-1) for financial support, F. Ziegs (IFW Dresden) for technical assistance, and Prof. L. Dunsch for his continuing support.

■ REFERENCES

(1) Bachilo, S. M.; Strano, M. S.; Kittrell, C.; Hauge, R. H.; Smalley, R. E.; Weisman, R. B. Structure-Assigned Optical Spectra of Single-Walled Carbon Nanotubes. *Science* **2002**, *298*, 2361−2366.

(2) O'Connell, M. J.; Bachilo, S. M.; Huffman, C. B.; Moore, V. C.; Strano, M. S.; Haroz, E. H.; Rialon, K. L.; Boul, P. J.; Noon, W. H.; Kittrell, C.; et al. Band Gap Fluorescence from Individual Single-Walled Carbon Nanotubes. *Science* **2002**, *297*, 593−596.

(3) Jingzhi Shang, Ma, L.; Li, J.; Ai, W.; Yu, T.; Gurzadyan, G. G. The Origin of Fluorescence from Graphene Oxide. *Sci. Rep.* **2012**, *2*, 792 DOI: 10.1038/srep00792.

(4) Luo, Z.; Vora, P. M.; Mele, E. J.; Johnson, A. T. C.; Kikkawa, J. M. Photoluminescence and Band Gap Modulation in Graphene Oxide. *Appl. Phys. Lett.* **2009**, *94*, 111909.

(5) Cao, L.; Meziani, M. J.; Sahu, S.; Sun, Y.-P. Photoluminescence Properties of Graphene versus Other Carbon Nanomaterials. *Acc. Chem. Res.* **2013**, *46*, 171−180.

(6) Zhu, S.; Tang, S.; Zhang, J.; Yang, B. Control the Size and Surface Chemistry of Graphene for the Rising Fluorescent Materials. *Chem. Commun.* **2012**, *48*, 4527−4539.

(7) Li, H.; Kang, Z.; Liu, Y.; Lee, S.-T. Carbon Nanodots: Synthesis, Properties And Applications. *J. Mater. Chem.* **2012**, *22*, 24230−24253.

(8) Yan, X.; Li, B.; Li, L.-s. Colloidal Graphene Quantum Dots with Well-Defined Structures. *Acc. Chem. Res.* **2013**, DOI: 10.1021/ar300137p.

(9) Shen, J.; Zhu, Y.; Yang, X.; Li, C. Graphene Quantum Dots: Emergent Nanolights For Bioimaging, Sensors, Catalysis and Photovoltaic Devices. *Chem. Commun.* **2012**, *48*, 3686−3699.

(10) Scholes, G. D.; Rumbles, G. Excitons in Nanoscale Systems. *Nat. Mater.* **2006**, *5*, 683−696.

(11) Dennler, G.; Scharber, M. C.; Brabec, C. J. Polymer−Fullerene Bulk-Heterojunction Solar Cells. *Adv. Mater.* **2009**, *21*, 1323−1338.

(12) Mroz, P.; Tegos, G. P.; Gali, H.; Wharton, T.; Sarna, T.; Hamblin, M. R. Photodynamic Therapy with Fullerenes. *Photochem. Photobiol. Sci.* **2007**, *6*, 1139−1149.

(13) Matsuo, Y.; Sato, Y.; Hashiguchi, M.; Matsuo, K.; Nakamura, E. Synthesis, Electrochemical and Photophysical Properties, and Electroluminescent Performance of the Octa- and Deca(aryl)[60]fullerene Derivatives. *Adv. Funct. Mater.* **2009**, *19*, 2224−2229.

(14) Orlandi, G.; Negri, F. Electronic States And Transitions in C_{60} and C_{70} Fullerenes. *Photochem. Photobiol. Sci.* **2002**, *1*, 289−308.

(15) Ma, B.; Sun, Y. P. Fluorescence Spectra and Quantum Yields of [60]Fullerene and [70]Fullerene under Different Solvent Conditions. A Quantitative Examination Using a near-Infrared-Sensitive Emission Spectrometer. *J. Chem. Soc., Perkin Trans. 2* **1996**, 2157−2162.

(16) Arbogast, J. W.; Darmanyan, A. P.; Foote, C. S.; Rubin, Y.; Diederich, F. N.; Alvarez, M. M.; Anz, S. J.; Whetten, R. L. Photophysical Properties of C_{60}. *J. Phys. Chem.* **1991**, *95*, 11−12.

(17) Arbogast, J. W.; Foote, C. S. Photophysical Properties of C_{70}. *J. Am. Chem. Soc.* **1991**, *113*, 8886−8889.

(18) Catalan, J.; Elguero, J. Fluorescence of C_{60} and C_{70}. *J. Am. Chem. Soc.* **1993**, *115*, 9249−9252.

(19) Kim, D. H.; Lee, M. Y.; Suh, Y. D.; Kim, S. K. Observation of Fluorescence Emission from Solutions of C_{60} and C_{70} and Measurement of Their Excited-State Lifetimes. *J. Am. Chem. Soc.* **1992**, *114*, 4429−4430.

(20) Shen, J.; Zhu, Y.; Yang, X.; Zong, J.; Zhang, J.; Li, C. One-Pot Hydrothermal Synthesis of Graphene Quantum Dots Surface-Passivated by Polyethylene Glycol and Their Photoelectric Conversion under Near-Infrared Light. *New J. Chem.* **2011**, *36*, 97−101.

(21) Zhu, S.; Meng, Q.; Wang, L.; Zhang, J.; Song, Y.; Jin, H.; Zhang, K.; Sun, H.; Wang, H.; Yang, B. Highly Photoluminescent Carbon Dots for Multicolor Patterning, Sensors, and Bioimaging. *Angew. Chem., Int. Ed. Engl.* **2013**, *52*, 3953−3957.
(22) Nakamura, Y.; Taki, M.; Tobita, S.; Shizuka, H.; Yokoi, H.; Ishiguro, K.; Sawaki, Y.; Nishimura, J. Photophysical Properties of Various Regioisomers of [60]Fullerene-*O*-quinodimethane Bisadducts. *J. Chem. Soc., Perkin Trans. 2* **1999**, 127−130.
(23) Sun, Y. P.; Lawson, G. E.; Riggs, J. E.; Ma, B.; Wang, N. X.; Moton, D. K. Photophysical and Nonlinear Optical Properties of [60]Fullerene Derivatives. *J. Phys. Chem. A* **1998**, *102*, 5520−5528.
(24) Ma, B.; Bunker, C. E.; Guduru, R.; Zhang, X. F.; Sun, Y. P. Quantitative Spectroscopic Studies of the Photoexcited State Properties of Methano- and Pyrrolidino-[60]Fullerene Derivatives. *J. Phys. Chem. A* **1997**, *101*, 5626−5632.
(25) Fujita, T.; Matsuo, Y.; Nakamura, E. Synthesis of Tetradeca- and Pentadeca(organo)[60]fullerenes Containing Unique Photo- and Electroluminescent π-Conjugated Systems. *Chem. Mater.* **2012**, *24*, 3972−3980.
(26) Schwell, M.; Gustavsson, T.; Marguet, S.; de la Vaissiere, B.; Wachter, N. K.; Birkett, P. R.; Mialocq, J. C.; Leach, S. The Fluorescence Properties of the Phenylated Fullerenes $C_{70}Ph_4$, $C_{70}Ph_6$, $C_{70}Ph_8$, and $C_{70}Ph_{10}$ in Room Temperature Solutions. *Chem. Phys. Lett.* **2001**, *350*, 33−38.
(27) Benasson, R. V.; Schwell, M.; Fanti, M.; Wachter, N. K.; Lopez, J. O.; Janot, J. M.; Birkett, P. R.; Land, E. J.; Leach, S.; Seta, P.; et al. Photophysical Properties of the Ground and Triplet State of Four Multiphenylated [70]Fullerene Compounds. *ChemPhysChem* **2001**, *2*, 109−114.
(28) Kareev, I. E.; Kuvychko, I. V.; Lebedkin, S. F.; Miller, S. M.; Anderson, O. P.; Seppelt, K.; Strauss, S. H.; Boltalina, O. V. Synthesis, Structure, and ^{19}F NMR Spectra of 1,3,7,10,14,17,23,28,31,40-$C_{60}(CF_3)_{10}$. *J. Am. Chem. Soc.* **2005**, *127*, 8362−8375.
(29) Kareev, I. E.; Kuvychko, I. V.; Popov, A. A.; Lebedkin, S. F.; Miller, S. M.; Anderson, O. P.; Strauss, S. H.; Boltalina, O. V. High-Temperature Synthesis of the Surprisingly Stable C_1-$C_{70}(CF_3)_{10}$ Isomer With A *Para*^{7}-*Meta*-*Para* Ribbon of Nine $C_6(CF_3)_2$ Edge-Sharing Hexagons. *Angew. Chem., Int. Ed.* **2005**, *44*, 7984−7987.
(30) Popov, A. A.; Kareev, I. E.; Shustova, N. B.; Lebedkin, S. F.; Strauss, S. H.; Boltalina, O. V.; Dunsch, L. Synthesis, Spectroscopic, and Electrochemical Characterization, and DFT Study of Seventeen $C_{70}(CF_3)_n$ Derivatives (n = 2, 4, 6, 8, 10, 12). *Chem.—Eur. J.* **2008**, *14*, 107−121.
(31) Dorozhkin, E. I.; Ignat'eva, D. V.; Tamm, N. B.; Goryunkov, A. A.; Khavrel, P. A.; Ioffe, I. N.; Popov, A. A.; Kuvychko, I. V.; Streletskiy, A. V.; Markov, V. Y.; et al. Synthesis, Characterization, and Theoretical Study of Stable Isomers of $C_{70}(CF_3)_n$ (n = 2, 4, 6, 8, 10). *Chem.—Eur. J.* **2006**, *12*, 3876−3889.
(32) Goryunkov, A. A.; Kuvychko, I. V.; Ioffe, I. N.; Dick, D. L.; Sidorov, L. N.; Strauss, S. H.; Boltalina, O. V. Isolation of $C_{60}(CF_3)_n$ (n = 2, 4, 6, 8, 10) with High Compositional Purity. *J. Fluor. Chem.* **2003**, *124*, 61−64.
(33) Popov, A. A.; Kareev, I. E.; Shustova, N. B.; Stukalin, E. B.; Lebedkin, S. F.; Seppelt, K.; Strauss, S. H.; Boltalina, O. V.; Dunsch, L. Electrochemical, Spectroscopic, and DFT Study of $C_{60}(CF_3)_n$ Frontier Orbitals (n = 2−18): The Link between Double Bonds in Pentagons and Reduction Potentials. *J. Am. Chem. Soc.* **2007**, *129*, 11551−11568.
(34) Kareev, I. E.; Popov, A. A.; Kuvychko, I. V.; Shustova, N. B.; Lebedkin, S. F.; Bubnov, V. P.; Anderson, O. P.; Seppelt, K.; Strauss, S. H.; Boltalina, O. V. Synthesis and X-ray or NMR/DFT Structure Elucidation of Twenty-One New Trifluoromethyl Derivatives of Soluble Cage Isomers of C_{76},C_{78},C_{84}, and C_{90}. *J. Am. Chem. Soc.* **2008**, *130*, 13471−13489.
(35) Shustova, N. B.; Kuvychko, I. V.; Bolskar, R. D.; Seppelt, K.; Strauss, S. H.; Popov, A. A.; Boltalina, O. V. Trifluoromethyl Derivatives of Insoluble Small-HOMO−LUMO-gap hollow higher fullerenes. NMR and DFT Structure Elucidation of C_2-(C_{74}-D_{3h})-$(CF_3)_{12}$, C_s-(C_{76}-T_d(2))$(CF_3)_{12}$, C_2-(C_{78}-D_{3h}(5))$(CF_3)_{12}$, C_s-(C_{80}-C_{2v}(5))$(CF_3)_{12}$, and C_2-(C_{82}-C_2(5))$(CF_3)_{12}$. *J. Am. Chem. Soc.* **2006**, *128*, 15793−15798.
(36) Tamm, N. B.; Sidorov, L. N.; Kemnitz, E.; Troyanov, S. I. Crystal Structures of $C_{94}(CF_3)_{20}$ and $C_{96}(C_2F_5)_{12}$ Reveal the Cage Connectivities in C_{94}(61) and C_{96}(145) Fullerenes. *Angew. Chem., Int. Ed. Engl.* **2009**, *48*, 9102−9104.
(37) Troyanov, S. I.; Tamm, N. B. Crystal and Molecular Structures of Trifluoromethyl Derivatives of Fullerene C_{86}, $C_{86}(CF_3)_{16}$, and $C_{86}(CF_3)_{18}$. *Crystallogr. Rep.* **2009**, *54*, 598−602.
(38) Troyanov, S. I.; Tamm, N. B. Cage Connectivities of C_{88}(33) and C_{92}(82) Fullerenes Captured as Trifluoromethyl Derivatives, $C_{88}(CF_3)_{18}$ and $C_{92}(CF_3)_{16}$. *Chem. Commun.* **2009**, 6035−6037.
(39) Kuvychko, I. V.; Spisak, S. N.; Chen, Y.-S.; Popov, A. A.; Petrukhina, M. A.; Strauss, S. H.; Boltalina, O. V. A Buckybowl with a Lot of Potential: C_5-$C_{20}H_5(CF_3)_5$. *Angew. Chem., Int. Ed. Engl.* **2012**, *51*, 4939−4942.
(40) Kuvychko, I. V.; Castro, K. P.; Deng, S. H. M.; Wang, X.-B.; Strauss, S. H.; Boltalina, O. V. Taming Hot CF_3 Radicals: Incrementally Tuned Families of Polyarene Electron Acceptors for Air-Stable Molecular Optoelectronics. *Angew. Chem., Int. Ed. Engl.* **2013**, *52*, 4871−4874.
(41) Li, Y.; Li, C.; Yue, W.; Jiang, W.; Kopecek, R.; Qu, J.; Wang, Z. Direct Functionalization of Polycyclic Aromatics via Radical Perfluoroalkylation. *Org. Lett.* **2010**, *12*, 2374−2377.
(42) Hamilton, C. E.; Lomeda, J. R.; Sun, Z.; Tour, J. M.; Barron, A. R. Radical Addition of Perfluorinated Alkyl Iodides to Multi-Layered Graphene and Single-Walled Carbon Nanotubes. *Nano Res.* **2013**, *3*, 138−145.
(43) Schmidt, B. M.; Seki, S.; Topolinski, B.; Ohkubo, K.; Fukuzumi, S.; Sakurai, H.; Lentz, D. Electronic Properties of Trifluoromethylated Corannulenes. *Angew. Chem., Int. Ed. Engl.* **2012**, *51*, 11385−11388.
(44) Kuvychko, I. V.; Whitaker, J. B.; Larson, B. W.; Raguindin, R. S.; Suhr, K. J.; Strauss, S. H.; Boltalina, O. V. Pressure Effect on Heterogeneous Trifluoromethylation of Fullerenes and Its Application. *J. Fluor. Chem.* **2011**, *132*, 679−685.
(45) Clements, A. F.; Haley, J. E.; Urbas, A. M.; Kost, A.; Rauh, R. D.; Bertone, J. F.; Wang, F.; Wiers, B. M.; Gao, D.; Stefanik, T. S.; et al. Photophysical Properties of C_{60} Colloids Suspended in Water with Triton X-100 Surfactant: Excited State Properties with Femtosecond Resolution. *J. Phys. Chem. A* **2009**, *113*, 6437−6445.
(46) Lembo, A.; Tagliatesta, P.; Guldi, D. M. Synthesis and Photophysical Investigation of New Porphyrin Derivatives with β-Pyrrole Ethynyl Linkage and Corresponding Dyad with [60]Fullerene. *J. Phys. Chem. A* **2006**, *110*, 11424−11434.
(47) Fraelich, M. R.; Weisman, R. B. Triplete States of C_{60} and C_{70} in Solution: Long Intrinsic Lifetimes and Energy Pooling. *J. Phys. Chem.* **1993**, *97*, 11145−11147.
(48) Hung, R. R.; Grabowski, J. J. C_{70}: Intersystem Crossing and Singlet Oxygen Production. *Chem. Phys. Lett.* **1992**, *192*, 249−253.
(49) Hope, M. J.; Higlett, M. P.; Andrews, D. L.; Meech, S. R.; Hands, I. D.; Dunn, J. L.; Bates, C. A. Observation of Ultrafast Internal Conversion in Fullerene Anions in Solution. *Chem. Phys. Lett.* **2009**, *474*, 112−114.
(50) Tanigaki, K.; Ebbesen, T. W.; Kuroshima, S. Picosecond and Nanosecond Studies of the Excited-State Properties of C_{70}. *Chem. Phys. Lett.* **1991**, *185*, 189−192.
(51) Ebbesen, T. W.; Tanigaki, K.; Kuroshima, S. Excited-State Properties of C_{60}. *Chem. Phys. Lett.* **1991**, *181*, 501−504.
(52) Strickler, S. J.; Berg, R. A. Relationship between Absorption Intensity and Fluorescence Lifetime of Molecules. *J. Chem. Phys.* **1962**, *37*, 814−822.
(53) Klan, P.; Wirz, J. *Photochemistry of Organic Compounds: From Concepts To Practice*; John Wiley & Sons Ltd: Chichester, U.K., 2009.
(54) Rurack, K.; Spieles, M. Fluorescence Quantum Yields of a Series of Red and Near-Infrared Dyes Emitting at 600−1000 nm. *Anal. Chem.* **2011**, *83*, 1232−1242.
(55) Dixon, J. M.; Taniguchi, M.; Lindsey, J. S. PhotochemCAD 2. A Refined Program with Accompanying Spectral Databases for Photochemical Calculations. *Photochem. Photobiol.* **2005**, *81*, 212−213.

(56) Prahl, S. Oregon Medical Laser Center. *Tetraphenylporphyrin*. http://omlc.ogi.edu/spectra/PhotochemCAD/html/099.html (accessed January 8, 2013).
(57) Laikov, D. N.; Ustynuk, Y. A. PRIRODA-04: A Quantum-Chemical Program Suite. New Possibilities in the Study of Molecular Systems with the Application of Parallel Computing. *Russ. Chem. Bull.* **2005**, *54*, 820−826.
(58) Laikov, D. N. Fast Evaluation of Density Functional Exchange-Correlation Terms Using the Expansion of the Electron Density in Auxiliary Basis Sets. *Chem. Phys. Lett.* **1997**, *281*, 151−156.
(59) Humphrey, W.; Dalke, A.; Schulten, K. VMD - Visual Molecular Dynamics. *J. Mol. Graphics* **1996**, *14*, 33−38.